Available online at www.sciencedirect.com
SCIENCE DIRECT
C. R. Mecanique 334 (2006) 285–291
COMPTES RENDUS MECANIQUE
http://france.elsevier.com/direct/CRAS2B/

Estimation of aerodynamic noise generated by forced compressible round jets

Mohamed Maidi [1]

Équipe MoST/LEGI, B.P. 53, 38041 Grenoble cedex 09, France

Received 10 March 2006; accepted 14 March 2006

Presented by Marcel Lesieur

Abstract

An acoustic numerical code based on Ligthill's analogy is combined with large-eddy simulations techniques in order to evaluate the noise emitted by subsonic ($M = 0.7$) and supersonic ($M = 1.4$) round jets. We show first that, for centerline Mach number $M = 0.9$ and Reynolds number $Re = 3.6 \times 10^3$, acoustic intensities compare satisfactorily with experimental data of the literature in terms of levels and directivity. Afterwards, high Reynolds number ($Re = 3.6 \times 10^4$) free and forced jets at Mach 0.7 and 1.4 are studied. Numerical results show that the jet noise intensity depends on the nature of the upstream mixing layer. Indeed, the subsonic jet is 4 dB quieter than the free jet when acting on this shear layer by superposing inlet varicose and flapping perturbations at preferred and first subharmonic frequency, respectively. The maximal acoustic level of the supersonic jet is, on the other hand, 3 dB lower than the free one with a flapping upstream perturbation at the second subharmonic. The results reported in this paper confirm previous works presented in the literature demonstrating that jet noise may be modified according to the inlet conditions. ***To cite this article: M. Maidi, C. R. Mecanique 334 (2006).***

Résumé

Estimation du bruit d'origine aérodynamique rayonné par des jets ronds forcés compressibles. Un code numérique d'acoustique basé sur l'analogie de Lighthill est combiné avec des simulations de grandes échelles de jets ronds compressibles, afin de déterminer le bruit rayonné par les jets subsoniques ($M = 0{,}7$) et supersoniques ($M = 1{,}4$). On montre d'abord que, pour un nombre de Mach de 0.9 et un nombre de Reynolds de $3{,}6 \times 10^3$, les intensités acoustiques ont un accord satisfaisant avec les données expérimentales de la littérature, en terme de niveaux et de directivité. On étudie ensuite des jets libres et forcés à des nombres de Mach de 0,7 et 1,4 et des nombres de Reynolds élevés ($Re = 3{,}6 \times 10^4$). Les résultats numériques montrent que l'intensité du bruit du jet dépend de l'état de la couche de mélange amont. En effet, le jet subsonique est 4 dB plus silencieux que le jet libre lorsque l'on manipule sa couche de mélange amont en superposant la combinaison d'une perturbation variqueuse et d'une alternée au mode préférentiel et sous-harmonique, respectivement. Au contraire, le niveau de bruit du jet supersonique est 3 dB plus faible que le jet libre avec une perturbation amont alternée au deuxième mode sous-harmonique. Les résultats obtenus confirment des travaux antérieurs présentés dans la littérature et montrant que le bruit des jets peut être modifié selon les conditions amont. ***Pour citer cet article : M. Maidi, C. R. Mecanique 334 (2006).***

E-mail address: M.Maidi@kingston.ac.uk (M. Maidi).

[1] Present address: Faculty of Engineering, Kingston University, Roehampton Vale, Friars Avenue, London SW15 3DW, UK.

1631-0721/$ – see front matter
doi:10.1016/j.crme.2006.03.006

Keywords: Computational fluid mechanics; Acoustics; Turbulence; Compressible jets control

Mots-clés : Mécanique des fluides numérique ; Acoustique ; Turbulence ; Contrôle de jets compressibles

Version française abrégée

Des lois strictes concernant l'environnement pour les aéroports proches des villes ont imposé des limitations sur le bruit des jets des turboréacteurs des avions de transport civil. Ces considérations constituent un facteur très important que les constructeurs aéronautiques doivent prendre en compte pour la conception des avions. Dans ce contexte, un effort considérable a été fait au cours des cinquante dernières années pour mieux comprendre les mécanismes physiques de génération de bruit dans les jets, dans l'espoir de le réduire au maximum.

Plusieur études expérimentales et numériques faites sur les écoulement associés aux jets ont montré que le développement amont a une influence importante sur la génération du bruit aérodynamique (Bishop et al. [1], Juvé et al. [2], Laufer et Yen [3], Bridges et Hussain [4], Simonich et al. [5]). Ces études ont lié le mécanisme de génération de bruit à la forme et la dynamique des tourbillons cohérents qui apparaissent dans la zone de transition du jet. Le contrôle de ces tourbillons primaires peut donc jouer un rôle important dans la réduction de bruit.

On se propose dans cette Note d'étudier les effets des perturbations amont sur le développement et l'intensité acoustique des jets ronds subsonique ($M = 0{,}7$) et supersoniques ($M = 1{,}4$) à un nombre de Reynolds de $3{,}6 \times 10^4$. Cette étude prolonge des travaux antérieurs sur le contrôle actif des jets compressibles (voir Maidi et al. [8], Maidi [9] et Lesieur et al. [10], pour plus de détail). Ces travaux ont souligné que la meilleure performance de contrôle du jet subsonique, en termes de plus grand taux d'élargissement et de mélange, est obtenue lorsqu'on excite sa couche de mélange amont en combinant une excitation variqueuse au mode préférentiel et une excitation alternée au premier mode sous-harmonique. En revanche, dans le cas supersonique, le taux d'élargissement le plus élevé est obtenu en utilisant une excitation alternée au deuxième mode sous-harmonique. La question posée, et à laquelle nous allons essayer de répondre maintenant, est de savoir si cette augmentation de la capacité de mélange du jet est associée à une réduction de la puissance sonore émise. La technique adoptée pour cette étude consiste à combiner un calcul aéroacoustique basé sur l'analogie de Lighthill avec un code de simulation des grandes échelles qui permet de calculer les champs aérodynamiques. Pour modéliser le bruit rayonné par le jet, nous avons considéré la solution intégrale (5) de l'équation de Lighthill (4) dans la région lointaine du domaine de calcul. Une expression de l'intensité acoustique est ainsi obtenue (6). L'évaluation du niveau sonore est effectuée pour des angle θ variant de 0 à 180° par rapport à la direction de l'écoulement et pour une distance de $60R$ à partir de la sortie de la tuyère d'éjection (R est le rayon amont du jet). Pour un nombre de Mach amont au centre de jet de 0,9 et un nombre de Reynolds de $3{,}6 \times 10^3$, la Fig. 3 montre que les niveaux sonores du jet forcé prédits par notre modèle d'acoustique sont en bon accord avec les données expérimentales de Stromberg et al. [16] avec les mêmes conditions amont. Nous évaluons ensuite le bruit des jets subsonique et supersonique à grand nombre de Reynolds. Les Figs. 4 (a) et (b) montrent les niveaux sonores produits par les jets libres et forcés subsoniques et supersoniques. On constate que le bruit des jets est prépondérant en aval et presente un maximum pour des angles d'observation θ compris entre 30 et 35°. Ce bruit est lié à la dynamique et l'appariement tourbillonnaire des grosses structures turbulentes qui apparaissent dans la zone de transition (Bogey et Bailly [6]). Sur ces deux figures, il est clair que, pour des angles d'observation inférieurs à 60°, les niveaux sonores du jet subsonique ont diminué nettement lorsqu'on excite sa couche de mélange amont en superposant une perturbation variqueuse harmonique et une perturbation alternée sous-harmonique. Le niveau maximal du bruit est ainsi diminué de 4 dB par rapport au jet libre, ce qui est assez significatif. Quant au jet supersonique, il est plus silencieux de 3 dB avec un forçage constitué d'une excitation alternée au deuxième mode sous-harmonique. Néanmoins, les niveaux calculés pour des angles supérieurs à 60° sont un peu plus élevés que dans le jet libre pour les deux cas des jets forcés.

1. Introduction

Strict environmental regulations concerning airports located close to cities have put strong limitations on the noise emitted by civilian aircrafts turbojet engines. These considerations constitute an important factor which aeronautical designers have to take into account early in planes conception. In this context, a considerable effort has been devoted, over the last fifty years, to better understand the physical mechanisms of jets noise generation, in the hope of reducing

their acoustic emission to the maximum. Various experiments showed that the upstream jet development has a great influence on noise generation (Bishop et al. [1], Juvé et al. [2], Laufer and Yen [3]). These authors have linked the noise generation mechanism to the shape and dynamics of coherent vortices present in the jet transitional region. Therefore, controlling these primary vortices by a proper manipulation of the mixing layer can play an important role for jet-noise reduction. Bridges and Hussain [4] have found experimentally that for a Reynolds number $Re_D = 1.5 \times 10^5$ and Mach number ranging from 0.15 to 0.35, a round jet was 2.5 dB quieter when tripping its upstream shear-layer. Using tabs in a round jet at $Re_D = 1.7 \times 10^6$, Simonich et al. [5] observed a decrease of sound levels by about 2 dB.

Recently, Bogey and Bailly [7] studied in detail with the aid of large-eddy simulations (LES) techniques the effects of inflow conditions on flow development and acoustic radiation of a high subsonic ($M = 0.9$), $Re_D = 4 \times 10^5$ round jet. The acoustic fields are obtained directly from the LES calculation without any approximation. Their results illustrate that jet noise may change according to the velocity fluctuations existing in the upstream mixing layer. Indeed, they found that reducing the inlet momentum thickness in a forced jet leads to an accelerated transition inducing an increase of turbulence intensities in the mixing layer. But more downstream, intensities decrease in the potential core. As a result, noise is respectively enhanced and reduced in the sideline and downstream directions.

In the present work, we investigate the effects of upstream perturbations on the development and acoustic radiation of subsonic ($M = 0.7$) and supersonic ($M = 1.4$) round jets at Reynolds number $Re_D = 3.6 \times 10^4$. The method of calculation is split into two parts. LES are first used to determine the aerodynamic flow fields in a given computing box. Then this box is inserted into a bigger computing domain, and the noise emission is calculated away from the jet using Ligthill's analogy. Although it is well known that this analogy is not exact (but not too bad, however), our motivation is to evaluate the ability of artificial inlet forcings to modify the jet acoustic emission.

In previous works, effects on the flow fields of different types of upstream forcing in subsonic (Mach 0.7) and supersonic (Mach 1.4) round jets have been investigated in detail with the aid of LES (see Maidi et al. [8], Maidi [9] and Lesieur et al. [10]). The LES code is a multi-domain compressible code of fourth-order accuracy in space and second-order in time. This code was intensively validated in round jet configurations (see Maidi and Lesieur [11] and Maidi [9]). All parameters of simulation can be found in [11] and [9]. The subgrid-scale model is the filtered structure-function model (FSF). All the simulations presented in this Note are performed with the same computational grid, which has $100 \times 74 \times 74$ points in the streamwise and transverse directions respectively. The computational domain is a parallelepipedic box of size $35 \times 20 \times 20$ nozzle radii respectively in the longitudinal and transverse directions. In order to correctly simulate the upstream jet mixing layer, the mesh is compressed in the y and z directions with a hyperbolic-tangent stretching. A correct formulation of the boundary conditions is important in computational aeroacoustics. In this context, non-reflecting boundary conditions are used at all sides of the domain. To avoid reflections, a sponge zone of length 17% of the computational domain length is added downstream.

2. Large-eddy simulations

In the present study, four simulations, selected from our earlier works on the study and control of compressible round jets (Maidi and Lesieur [11] and Maidi et al. [8]), are considered. This is summarized in Table 1. Besides the Mach number, principal differences between the various simulations come from the inlet velocity profile used as inflow boundary condition. In general, the shape of this profile is given by

$$\vec{U}(\vec{x}_0, t) = \vec{U}_m(\vec{x}_0) + \vec{U}_{\text{forc}}(\vec{x}_0, t) \tag{1}$$

Table 1
Details of large-eddy simulations presented

Tableau 1
Détails des simulations des grandes échelles présentées

Simulation	Mach	Reynolds	Forcing
LES_{nat1}	0.7	36 000	Natural
LES_{nat2}	1.4	36 000	Natural
LES_{for1}	0.7	36 000	Varicose-flapping excitation
LES_{for2}	1.4	36 000	Flapping excitation

where $\vec{x}_0 = (x = 0, y, z)$ is the inlet plane and t the simulation time. $\overrightarrow{U}_m(\vec{x}_0) = (U_m, 0, 0)$ represents the mean velocity vector which is given by a hyperbolic-tangent profile describing an annular shear layer of diameter D and momentum thickness θ_0. In order to initiate the turbulence, an additional white noise is imposed on the three upstream mean velocity components in the shear-layer gradient zone. The maximum intensity of the random noise in our simulations is set to 1.0% of the inlet maximum velocity. The term $\overrightarrow{U}_{\text{forc}}(\vec{x}_0, t)$ in Eq. (1) represents the upstream additional forcing. Two types of forcing, which led to the highest mixing rate, are considered here. The first excitation, named *flapping excitation*, is similar to that employed by Urbin and Métais [12] but at second subharmonic frequency.

$$U_{\text{forc}}(\vec{x}_0, t) = \varepsilon U_1 \sin\left(2\pi \frac{St_D^0}{4} \frac{U_1 t}{D}\right) \sin\left(\frac{2\pi y}{D}\right) \tag{2}$$

in which U_1 is the jet upstream centerline velocity and St_D^0 the forcing Strouhal number. Here St_D^0 is taken equal to 0.39 in the subsonic jet and 0.44 in the supersonic jet. The second type of excitation is of the varicose-flapping type, and consists in the combination of fundamental varicose and subharmonic flapping perturbations, similarly to that used by Danaila and Boersma [13] and Silva and Métais [14] in their incompressible simulations

$$U_{\text{forc}}(\vec{x}_0, t) = \varepsilon U_m(\vec{x}_0) \sin\left(\frac{2\pi St_D^0 U_1 t}{D}\right) + \varepsilon U_m(\vec{x}_0) \sin\left(2\pi \frac{St_D^0}{2} \frac{U_1 t}{D} + \frac{\pi}{4}\right) \cos(\phi) \left(\frac{2r}{D}\right) \tag{3}$$

where $r = \sqrt{y^2 + z^2}$ is the radial distance from the jet axis and ϕ is the azimuthal angle. These forcing are superimposed to the weak random white noise in the upstream mixing-layer zone. The relative amplitude of the forcing with respect to the inlet velocity is set $\varepsilon = 5\%$. Note that there is no forcing on the transverse velocity components.

The effect of these two forcings on the jet dynamics is documented in detail in Maidi et al. [8]. it was found that the highest spreading rate of the subsonic jet (Mach 0.7) is obtained with inlet varicose-flapping perturbations at preferred and first subharmonic frequencies, respectively (Fig. 1). In the supersonic jet (Mach 1.4), on the other hand, the maximal spreading rate is found with flapping excitation at second subharmonic frequency (Fig. 2).

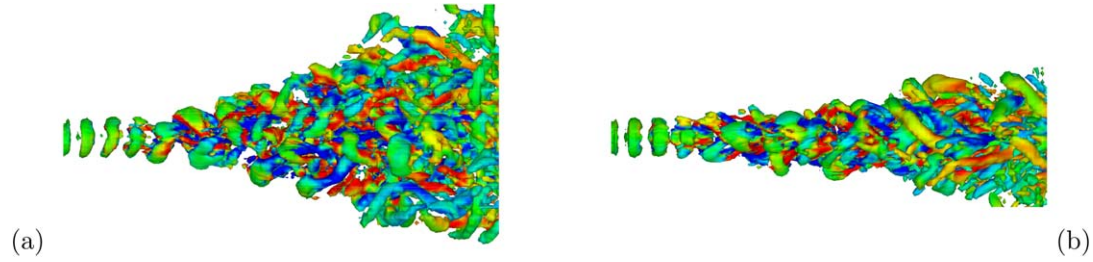

Fig. 1. Isosurfaces of positive Q (grey) coloured by the streamwise vorticity Ω_x (black) for the simulation LES_{for1}. The threshold is $0.20(U_1/D)^2$. (a) View in bifurcating plane; (b) view in bisecting plane. The bifurcating plane is defined as the plane containing the jet axis and the y direction. The plane perpendicular to the bifurcating plane and containing the jet axis is the bisecting plane (see Maidi et al. [8]).

Fig. 1. Isosurfaces de Q positif (gris) colorées par la vorticité longitudinale Ω_x (noir) pour la simulation LES_{for1}. Le seuil est de $0{,}20(U_1/D)^2$. (a) Vue sur le plan de bifurcation ; (b) vue sur le plan de bissection.

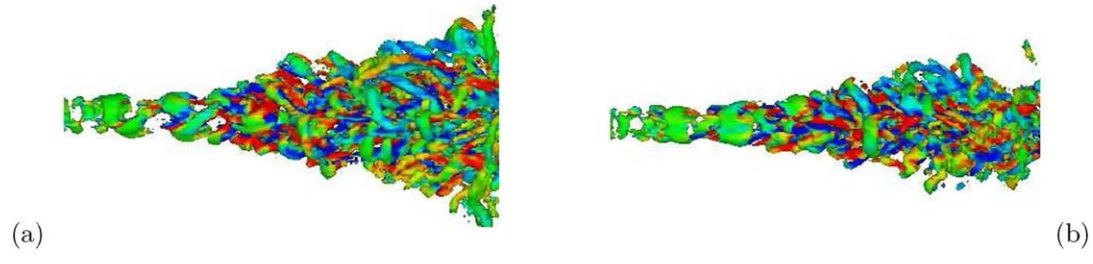

Fig. 2. Isosurfaces of positive Q (grey) coloured by the streamwise vorticity Ω_x (black) for the simulation LES_{for2}. The threshold is $0.20(U_1/D)^2$. (a) View in bifurcating plane; (b) view in bisecting plane.

Fig. 2. Isosurfaces de Q positif (gris) colorées par la vorticité longitudinale Ω_x (noir) pour la simulation LES_{for2}. Le seuil est de $0{,}20(U_1/D)^2$. (a) Vue sur le plan de bifurcation ; (b) vue sur le plan de bissection.

3. Lighthill's analogy

The acoustic field is evaluated utilizing Lighthill's theory (Lighthill [15]). Lighthill's equation describes the evolution of small acoustic density fluctuation ρ' in a quiescent flow and can be written as

$$\frac{\partial^2 \rho'}{\partial t^2} - c_0^2 \Delta \rho' = \frac{\partial^2 T_{ij}}{\partial x_i \partial x_j} \tag{4}$$

where $T_{ij} = \rho u_i u_j + (p' - c_0^2 \rho')\delta_{ij} - \tau_{ij}$ is Lighthill stress tensor, c_0 is the ambient sound speed and τ_{ij} is the viscous stress. To estimate the sound radiated by a finite domain of turbulent flow, Lighthill expressed the acoustic pressure at point $\vec{x}$ as a function of the tensor T_{ij} in the volume of turbulence V

$$p'(\vec{x}, t) = \frac{1}{4\pi} \frac{\partial^2}{\partial x_i \partial x_j} \int_V \frac{1}{r} T_{ij}\left(\vec{y}, t - \frac{r}{c_0}\right) \mathrm{d}\vec{y} \tag{5}$$

where $r = |\vec{x} - \vec{y}|$ is the distance between a point on the volume and an observer location. Note that Lighthill's tensor T_{ij} is evaluated at the retarded time $t - r/c_0$. This formulation permits to compute the near- and far-field sound of turbulence. The sound pressure level is then defined as

$$SPL = 20 \log_{10}\left(\frac{(\langle p'^2 \rangle)^{0.5}}{\rho_0 c_0}\right) \tag{6}$$

where the brackets $\langle\ \rangle$ denote the statistical mean.

4. Combination of Lighthill analogy and LES code

According to Eqs. (5) and (6), the numerical estimation of sound pressure levels requires the evaluation of instantaneous pressure data in the volume of turbulence. Our methodology was first to compute the different instantaneous flow fields using LES code and second to use these instantaneous data to estimate the sound pressure levels in various observer locations. Indeed, the LES computational domain is inserted into a bigger computing domain in which the observer locations are positioned on a circular arc at $60R$ (60 jet radii) from the nozzle exit. The noise evaluation is then carried out by considering a wave equation for ρ' outside the LES domain. The pressure fluctuations are estimated by using a numerical integration on the volume of turbulence (V) which is limited by the computational box. Here, we use a Gauss-Quadrature method of second order. It should be noticed that in the case of this study, we are limited to the case of isentropic flows with $p' = \rho' c_0^2$. Moreover, except for the validation case, the jet simulations are performed for a relatively high Reynolds number ($Re = 3.6 \times 10^4$) in which the viscous stress (τ_{ij}) can be neglected. In these assumptions, the Lighthill stress tensor can be written as:

$$T_{ij} \approx \rho u_i u_j \tag{7}$$

5. Results

First we validate our acoustic code by comparisons with a forced-jet experiments of Stromberg et al. [16] at $M = 0.9$ and $Re = 3.6 \times 10^3$. The upstream velocity profile is the same as Freund et al. [17]

$$U(\vec{x}_0, t) = U_m(\vec{x}_0) + U_{\text{for}}(\vec{x}_0, t) \tag{8}$$

The upstream forcing $U_{\text{for}}(\vec{x}_0, t)$ is now defined as

$$U_{\text{for}}(\vec{x}_0, t) = \varepsilon U_m(\vec{x}_0) \sin(St_D.t) \tag{9}$$

in which $St_D = fD/U_1 = 0.45$ is the forcing Strouhal number and $\varepsilon = 0.0025$ the amplitude. There is no forcing on the transverse velocity components.

Because of this low Reynolds number, the viscous stress τ_{ij} in Lighthill equation (4) is here considered.

Fig. 3 shows the predicted far-field sound pressure level and levels measured by Stromberg et al. [16]. The observer locations for which SPLs are presented are located in a $60R$ radius arc. Here, R is the upstream jet radius. As can be

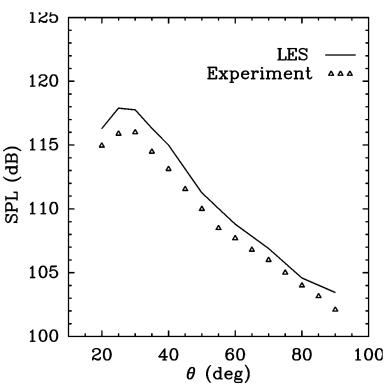

Fig. 3. Overall sound pressure levels at $60R$ from the jet nozzle, as a function of the observation angle θ.

Fig. 3. Niveaux sonores à une distance de $60R$ de la sortie de la buse, en fonction de l'angle d'observation θ.

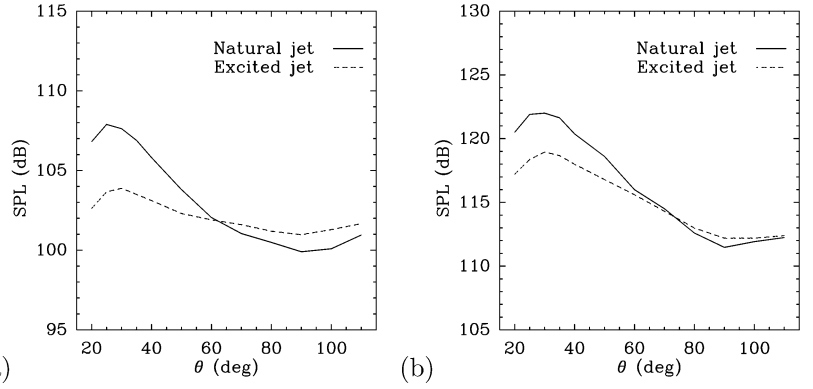

Fig. 4. Overall sound pressure levels at $60R$ from the jet nozzle, as a function of the observation angle θ. (a) Subsonic jet ($M = 0.7$); (b) supersonic jet ($M = 1.4$).

Fig. 4. Niveaux sonores à une distance de $60R$ de la sortie de la buse, en fonction de l'angle d'observation θ. (a) Jet subsonique ($M = 0,7$) ; (b) jet supersonique ($M = 1,4$).

seen in Fig. 3, predicted levels agree well with experimental data. Nevertheless there are some differences, especially for observer's angles below 40°. This can be attributed to the assumption taken in the section (4) in which the entropy term $\delta_{ij}(p' - c_o^2\rho')$ in Lighthill tensor is neglected. This does not represent a real jet flow but only gives a good approximation. Moreover, the Lighthill equation (4) describes the propagation of small acoustic density fluctuation in quiescent homogeneous flow. Such refractions, which are caused by the jet spreading close to the boundaries, are not taken into account by the present model. This may slightly modify the acoustic levels for low observation angles.

Now we study situations with $M = 0.7$ and $M = 1.4$ at Reynolds number $Re = 3.6 \times 10^4$. Fig. 4(a) represents the sound pressure levels located on a circular arc of $60R$ from the jet nozzle for both natural and excited subsonic round jets (simulations LES_{nat1} and LES_{for1}). The forcing used in this case corresponds to the varicose-flapping perturbations at preferred and first subharmonic frequencies, respectively. It is clear that for both free and excited jets, the acoustic levels are dominated downstream by low observation angles ($\theta < 60°$). The maximal level is located at about $\theta = 30°$. The maximum acoustic level turns out to be 4 dB lower for the excited jet than for the free jet. Since the noise emitted at this particular angle is linked to the vortex pairing at the end of the potential core (Bogey and Bailly [6]), the present result suggests that the vortex pairing noise can be reduced by acting on the large-scale structure at the nozzle exit. At larger observer angles ($\theta > 60°$), on the other hand, the acoustic levels of forced jet exceed slightly those of the natural jet.

The sound pressure levels evaluated for natural and excited supersonic jets are presented in Fig. 4(b). The maximal sound pressure level is now 3 dB lower with this flapping excitation at the second subharmonic frequency. Moreover, for large observation angles ($\theta > 60°$) the levels seem to be weakly affected by the forcing.

The present results are in agreement with numerical investigations of Bogey and Bailly [7] and experiments of Zaman [18] which show that the jet noise mechanisms depend strongly on the upstream mixing layer state. Our work shows that the jet noise may be reduced significantly in practice if the same type of upstream perturbations we use may be implemented in real engine configurations.

6. Conclusion

In this Note we have used Lighthill's analogy to evaluate the acoustic intensities of subsonic and supersonic round jets simulated by large-eddy simulations. Our objective was to show the feasibility of appropriate upstream forcings to reduce the acoustic noise by proper manipulations of large-scale vortices at the nozzle exit.

The noise levels and directivities are shown to depend appreciably on the upstream parameters and inlet conditions imposed at the jet inflow. The levels of downstream noise (for $\theta < 60°$) are shown to decrease when manipulating the subsonic jet shear layer with the superposition of varicose and flapping perturbations at the preferred and sub harmonic frequency, respectively. The maximal acoustic level is, indeed, reduced by 4 dB. The maximal noise level

of supersonic jets is reduced by 3 dB with a flapping upstream excitation at the second subharmonic frequency. Our results show also that the sideline levels (for $\theta > 60°$) of both subsonic and supersonic jets are enhanced by the forcing.

Acknowledgements

This work was sponsored by the French RRIT "Recherche Aéronautique sur le Supersonique" (Ministère de la Recherche). The author thanks P. Begou for his technical support.

References

[1] K.A. Bishop, J.E. Ffowcs Williams, W. Smith, On the noise sources of the unsuppressed high-speed jet, J. Fluid Mech. 50 (1971) 21–31.
[2] D. Juvé, M. Sunyach, G. Comte-Bellot, Intermittency of the noise emission in subsonic cold jets, J. Sound & Vib. 71 (3) (1980) 319–332.
[3] J. Laufer, T. Yen, Noise generation by a low-Mach-number jet, J. Fluid Mech. 134 (1983) 1–31.
[4] J.E. Bridges, K.M.F. Hussain, Roles of initial conditions and vortex pairing in jet noise, J. Sound & Vib. 117 (2) (1987) 289–311.
[5] J.C. Simonich, S. Narayanan, T.J. Barber, M.B. Nishimura, Aeroacoustic characterization, noise reduction, and dimensional scaling effects of high subsonic jets, AIAA Journal 39 (11) (2001) 2062–2069.
[6] C. Bogey, C. Bailly, Downstream subsonic jet noise: link with vortical structures intruding into the jet core, C. R. Mecanique 330 (2002) 527–533.
[7] C. Bogey, C. Bailly, Effects of inflow conditions and forcing on a Mach 0.9 jet and its radiated noise, AIAA Journal 43 (5) (2005) 1000–1007.
[8] M. Maidi, M. Lesieur, O. Métais, Vortex control in large-eddy simulations of compressible round jets, Journal of Turbulence (2005), in press.
[9] M. Maidi, Étude et contrôle des jets ronds compressibles par simulations des grandes échelles, PhD thesis, Grenoble (2004).
[10] M. Lesieur, O. Métais, P. Comte, Large-Eddy Simulations of Turbulence, Cambridge Univ. Press, Cambridge, UK, 2005.
[11] M. Maidi, M. Lesieur, Large-eddy simulations of spatially-growing subsonic and supersonic turbulent round jets, Journal of Turbulence 6 (38) (2005) 1–20.
[12] G. Urbin, O. Métais, Large-eddy simulations of three-dimensional spatially-developing round jets, in: P.R. Chollet, J.P. Voke, L. Kleiser (Eds.), Direct and Large-Eddy Simulations II, Kluwer Academic Publishers, Boston, MA, 1997, pp. 539–542.
[13] I. Danaila, B.J. Boersma, Direct numerical simulation of bifurcating jets, Phys. Fluids A 12 (2000) 1255–1257.
[14] C.B. da Silva, O. Métais, Vortex control of bifurcating jets: a numerical study, Phys. Fluids 14 (2002) 3798–3819.
[15] M.J. Lighthill, On the sound generated aerodynamically I. General theory, Proc. Roy. Soc. A 221 (1952) 564–587.
[16] J.L. Stromberg, D.K. Mclaughlin, T.R. Troutt, Flow field and acoustic properties of a Mach number 0.9 jet at low Reynolds number, J. Sound & Vib. 72 (1980) 159–176.
[17] J.B. Freund, S.K. Lele, P. Moin, Acoustic sources in a turbulent jet: a direct numerical simulation study, AIAA paper 99-1858 (1999).
[18] K.B.M.Q. Zaman, Flow field and near and far sound field of a subsonic jet, J. Sound & Vib. 106 (1986) 1–16.